Silicon (2019) 11:1401–1411
https://doi.org/10.1007/s12633-018-9943-8

ORIGINAL PAPER

Synthesis and Characterization of Hollow Mesoporous Silica Spheres and Studying the Load and Release of Dexamethasone

M. Amin Al Roaya[1] · F. Manteghi[1] · M. Haghverdi[1]

Received: 30 March 2017 / Accepted: 29 June 2018 / Published online: 20 July 2018

Abstract
Hollow mesoporous silica (HMS) spheres were synthesized using cetyltrimethylammonium bromide (CTAB) and carbon nanospheres as a hard template through a hydrothermal procedure. The prepared HMS was characterized by UV-Vis, FT-IR, TG, XRD, BET and SEM measurements. HMS was functionalized using aminopropyltriethoxysilane (APTES) and amino groups were linked on its surface. Synthesized mesoporous material consists of homogenous particles with a size about 500-600 nm. Channels on the shell have hexagonal arrangements. In comparison with MCM41 and SBA15, spherical HMS provides more volume for drug loading, for its hollow cores. Thereby, the ability of obtained mesoporous materials to load and release of dexamethasone as a drug was studied.

Keywords Hollow mesoporous silica (HMS) · Carbon nanospheres · Dexamethasone · Drug release

1 Introduction

Future nanotechnology hinges on the ability to synthesize new nanomaterials possessing distinct structural and functional features. Among them, hollow nanospheres possess "tunable" void volume, excellent flow performance, and large surface area [1]. Also, Hollow micro/nanostructural materials are a large family of functional materials and have attracted much research and industrial interest due to their special shape, low density, and large fraction of voids, large hollow cavities, intact shells, and uniform morphologies [2]. There have been reports about synthesis of silica hollow spheres by several methods such as sonochemical, solid particle templates, surfactant/vesicle templates, and emulsion templating technology. However, only several reports have occasionally involved the synthesis of hollow spheres with ordered porous wall structures. Moreover, their particles sizes are usually not uniform [3]. Previously, mesoporous hollow spheres have been synthesized by self-assembly of silica precursors with surfactant templates at oil−water, or air−water droplet interfaces, or using the vesicle approach. As these soft templates generally represent low stability and poor uniformity in solution, the obtained hollow materials are often ill-defined in shape and poly-dispersed in size. Also, the hollow core size and shell thickness cannot be easily and independently controlled by these techniques. To overcome these problems, the hard templating methods have been used to fabricate mesoporous silica hollow spheres by using polymer or inorganic beads as sacrificial core templates [4]. During the past three decades, controllable drug release system which can deliver the therapeutic drugs to the targeted cells or tissues in a controlled manner and enhanced drug efficiency with reduced toxicity has attracted much attention. So far, a large variety of materials, such as biodegradable polymers, hydroxyapatite, calcium phosphate cement, hydrogels, and mesoporous silica have been employed in controlled drug release systems [5]. It has been speculated that HMS spheres are more suitable as drug carriers compared to the conventional mesoporous silica, because HMS spheres exhibit the similar drug release kinetics, but hollow cores provide more volume for drug loading. Therefore, many efforts have been made to develop drug release systems based on the HMS spheres as carriers [6]. Recently, there has been a growing interest in synthesizing HMS with penetrating channels from the wall surface to its hollow core, and its in vitro drug release performances have also been studied. Compared to conventional

✉ F. Manteghi
f_manteghi@iust.ac.ir

[1] Department of Chemistry, Iran University of Science and Technology, Tehran, 1684613114, Iran

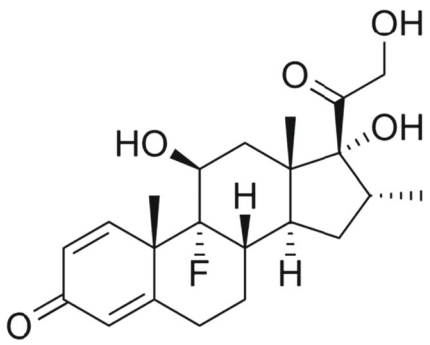

Scheme 1 Chemical structure of dexamethasone

solid porous materials, these hollow spheres show higher adsorption capacity for the drug molecules, which are also favorable for applications in confined nanocatalysts, biosensors, targeted drug and gene release, enzyme encapsulation, and nanoreactors [7].

In this work, we have prepared HMS spheres using CTAB and carbon nanospheres as a hard template to achieve spherical morphology. HMS was functionalized using aminopropyltriethoxysilane (APTES) and the load and release of dexamethasone drug (Scheme 1) on the product was studied.

2 Experimental Section

2.1 Materials and Reagents

Cetyltrimethylammonium bromide (CTAB), tetraethoxysilane (TEOS), 3-aminopropyltriethoxysilane (APTES), ammonium hydroxide (28.0-30.0%), ethanol, hydrochloric acid, nitric acid, glucose monohydrate, acetone and acetonitrile were purchased from Merck. All materials were used as obtained without further purification.

2.1.1 Preparation of Carbon Nanospheres by Hydrothermal Method

Glucose monohydrate (4.752 g) was dissolved in distilled water (60 mL) and stirred by magnetic stirrer. Then, it was placed in an autoclave for 12 h at 180 °C. After a while, a two-phase solution was formed that was brown in color. In order to separate the unreacted monomers and solvent, sample was centrifuged for 15 minutes at a speed of 6000 rpm. Then, ethanol was added to it and placed in an ultrasonic bath for 20 minutes. This cycle is called centrifuge-ultrasonic-washing and the cycle was repeated ten times using double distilled water and ethanol. After that, obtained mixture was placed in a 70 °C oven.

2.1.2 Synthesis of SiO_2 Hollow Nanospheres with the Carbon Core

At First, carbon template (100 mg) and cetyltrimethylammonium bromide (CTAB) (170 mg) were added to distilled water (30 mL) and dispersed for 30 minutes in an ultrasonic bath. Then, ethanol (13 mL) and ammonia (28 wt%, 0.45 mL) were added and redispersed for 30 minutes. After that, tetraethylorthosilicate (TEOS) (0.3 mL) was added dropwise and resulted solution dispersed for 2 h. It was filtered by centrifuge and washed six times using ethanol and double

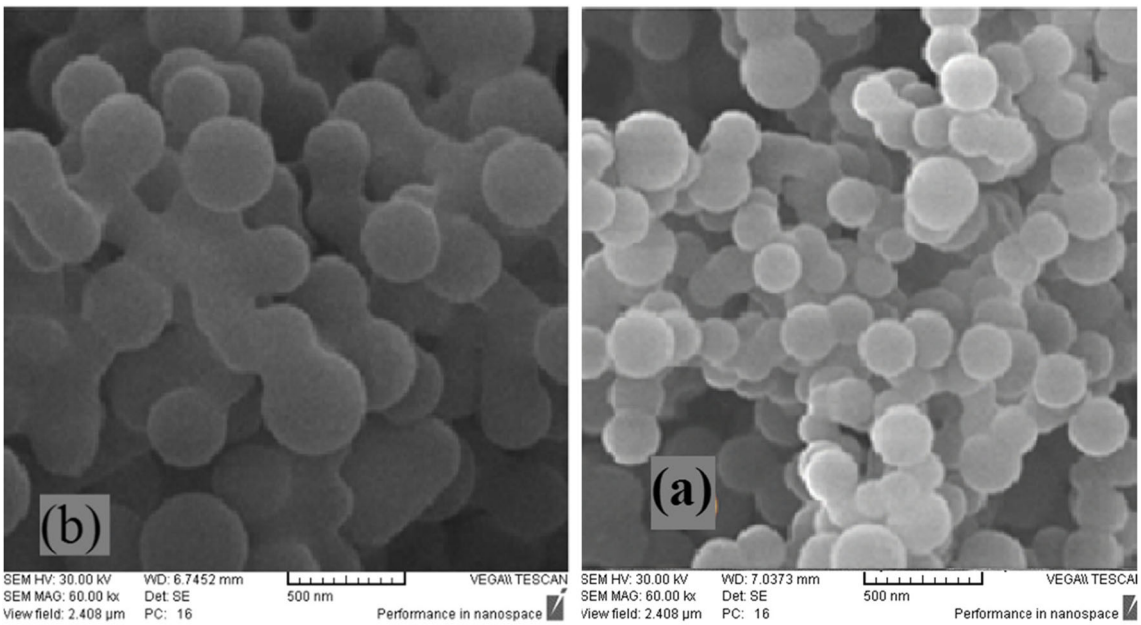

Fig. 1 SEM images of carbon nanospheres obtained from glucose **a** 0.4 M and **b** 0.6 M

distilled water. The pH of solution was 7 by washing. In order to remove the solvent, the final product was placed in an oven at 80 °C. Finally, for calcination and removal of the carbon core, the obtained precipitate was placed in a furnace at 500 °C with the rate of 2 °C/min.

2.1.3 Preparation of SiO_2 Nanoparticle Modified with Aminopropyltriethoxysilane (APTES)

Aminopropyltriethoxysilane (1mL) was transferred to a flask (50 mL) containing toluene (30 mL) and equipped to refrigerant. Then, SiO_2 hollow nanospheres (1 g) were added to balloon and the mixture refluxed under nitrogen atmosphere for 24 h. After completion of the reaction, the product is separated by centrifuge and washed with methanol. Finally, the product was placed in a 100 °C oven.

2.1.4 Preparation of Simulated body Fluid (SBF)

At first, the container including double distilled water (960 mL) and sodium chloride (6.5456 g) was stirred for 3 minutes at room temperature. Then, Sodium bicarbonate (2.2682 g), potassium chloride (0.3730 g) and disodium phosphate (0.1419 g) were added to it and stirred for 3 minutes. The solution was heated at 37 °C. After that, magnesium chloride hexahydrate (0.3049 g) was added

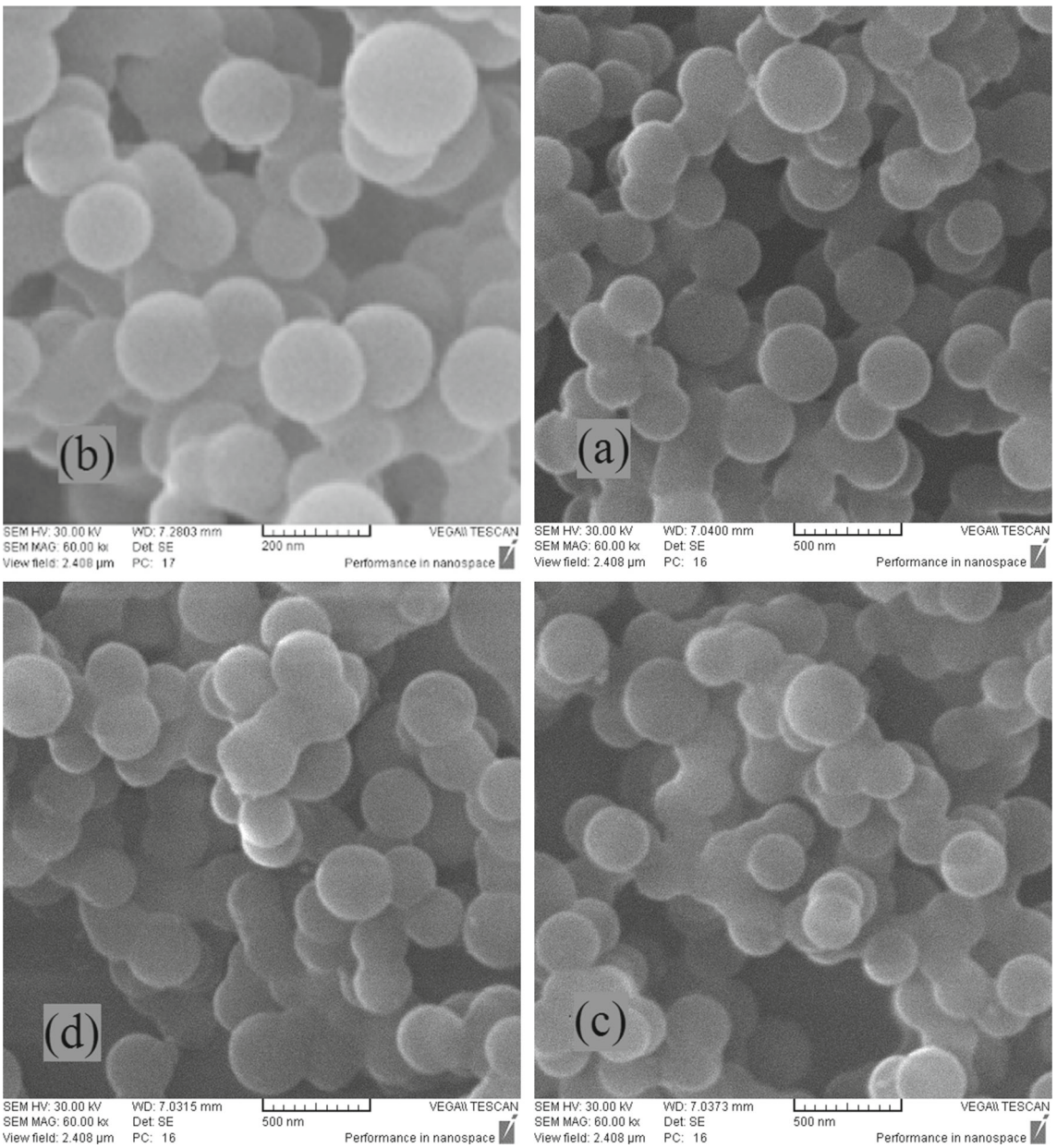

Fig. 2 SEM images of carbon nanospheres (0.4 M) in the times **a** 8, **b** 12, **c** 14 and **d** 16 h

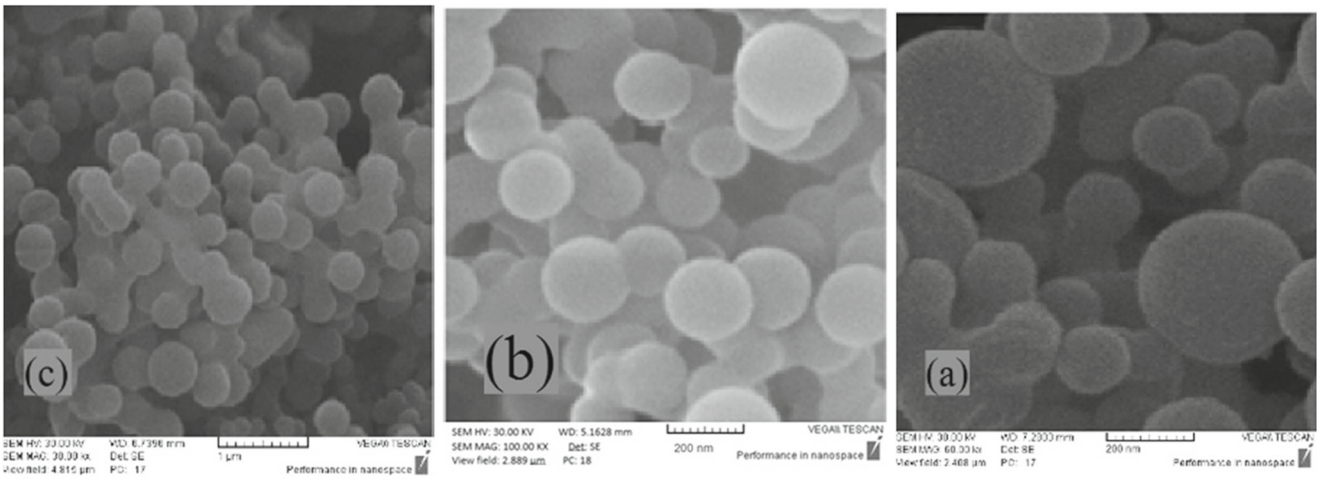

Fig. 3 SEM images of carbon nanospheres at temperatures: **a** 150, **b** 180 and **c** 210°C

to it and the solution was stirred for 3 minutes. Then hydrochloric acid (9 mL, 1 M) was added drop wise and again stirred for 3 minutes. Calcium chloride (0.3675 g) and sodium sulfate (0.071 g) were added and stirred for 3 minutes. Finally, trishydroxymethylaminomethane (6.057 g) was added to the solution and immediately the solution became dull. On stirring at 37 °C, the pH of solution reached to 7.4 by adding hydrochloric acid (30 mL, 1 M). Finally, the color of solution turned transparent and the resulting solution (SBF) was kept in a refrigerator at 4 °C [8].

2.1.5 Absorption of Drug by Hollow and Porous Nanospheres

The drug used in this research was dexamethasone and its structure was given in Scheme 1. At first, the solution of drug (250 ppm) was prepared and poured in the two separate containers. To one of them was added SiO_2 nanoparticles and to another SiO_2 nanoparticles modified with aminopropyltriethoxysilane was added and the mixture stirred. In order to evaluate the absorption of the drug, every

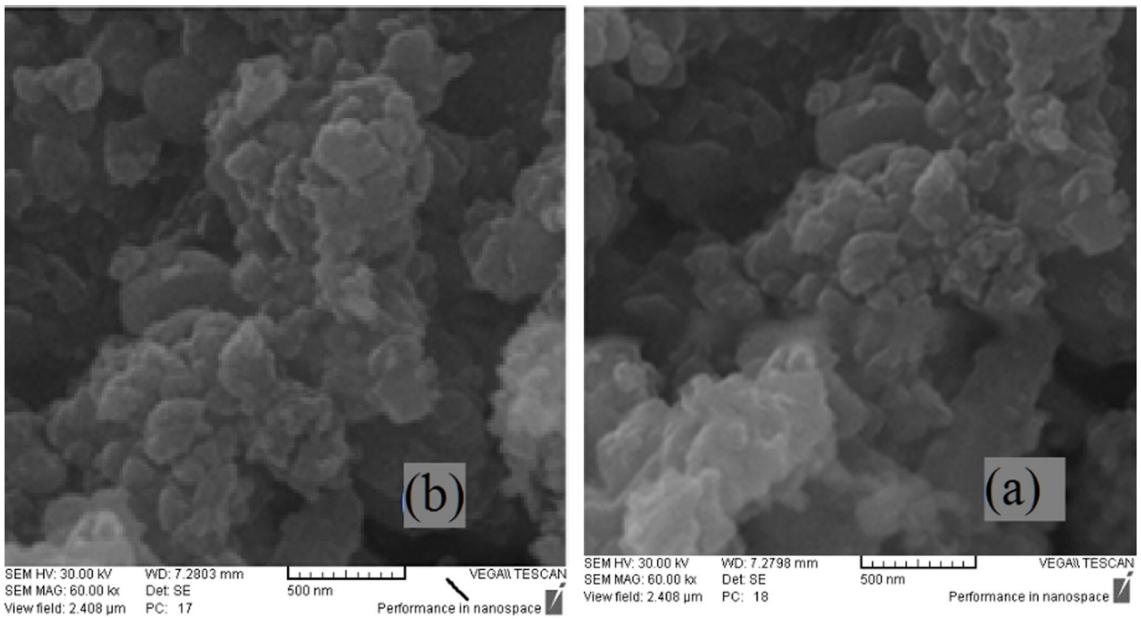

Fig. 4 SEM images after calcination of C@SiO_2 at **a** 650 and **b** 600 °C

6 hours, the mixture of drugs and nanospheres were sampled for 10 min and centrifuged at 14,000 rpm.

2.1.6 Drug Release from Nanospheres Loaded in Simulated Body Fluid

In this study, the drug was allowed to place in the vicinity of nanospheres for 72 hours. Then, using centrifuge, nanospheres were separated from the drug solution. After separating the hollow nanospheres, to obtain the loaded drug, was taken UV-Vis absorption spectrum from the remaining solution of the drug. Then, the loaded nanospheres were washed using deionized water and the final product dried in a vacuum oven for 4 h at 50 °C. After that, obtained nanospheres was poured in SBF (100 mL) and at the onset of drug release, sampled at 30 minutes, 1, 2, 5, 8 and 24 h, respectively. After centrifuging the samples, UV-Vis absorption spectra were measured in the range 190 to 800 nm.

2.2 Instrumentation

Powder X-ray diffraction (PXRD) patterns were measured on a JEOL diffractometer with monochromatized Cu Kα radiation ($\lambda = 1.5418$ Å) [9]. Thermogravimetric analysis (TGA) was carried out with a STA-409 PC Luxx. The N_2 adsorption/desorption isotherms were acquired at liquid nitrogen temperature (77 K) using a Belsorp mini II instrument, and the specific surface area was calculated by the Brunauer- Emmett-Teller (BET) method. The pore size distribution was determined using the Barret-Joner-Halenda (BJH) method [10]. The UV-Vis absorption spectra

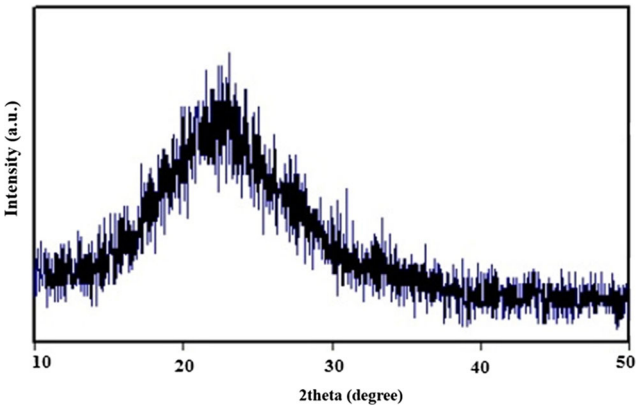

Fig. 6 XRD pattern of SiO_2 nanospheres

were acquired using a Shimadzu, mini 1240 single beam. Scanning electron microscopy (SEM) images were obtained on a LEO-1455 VP with gold coating. Fourier transform infrared (FT-IR) spectra were recorded on a Shimadzu-8400S spectrometer in the range of 450–4000 cm^{-1} using KBr pellets [11].

3 Results and Discussion

3.1 SEM Images of Carbon Nanospheres

The effect of parameters such as concentration, time and temperature on the morphology and size of the nanospheres and also uniform size distribution of the nanospheres were examined. The claim can be proved with SEM images obtained from different samples.

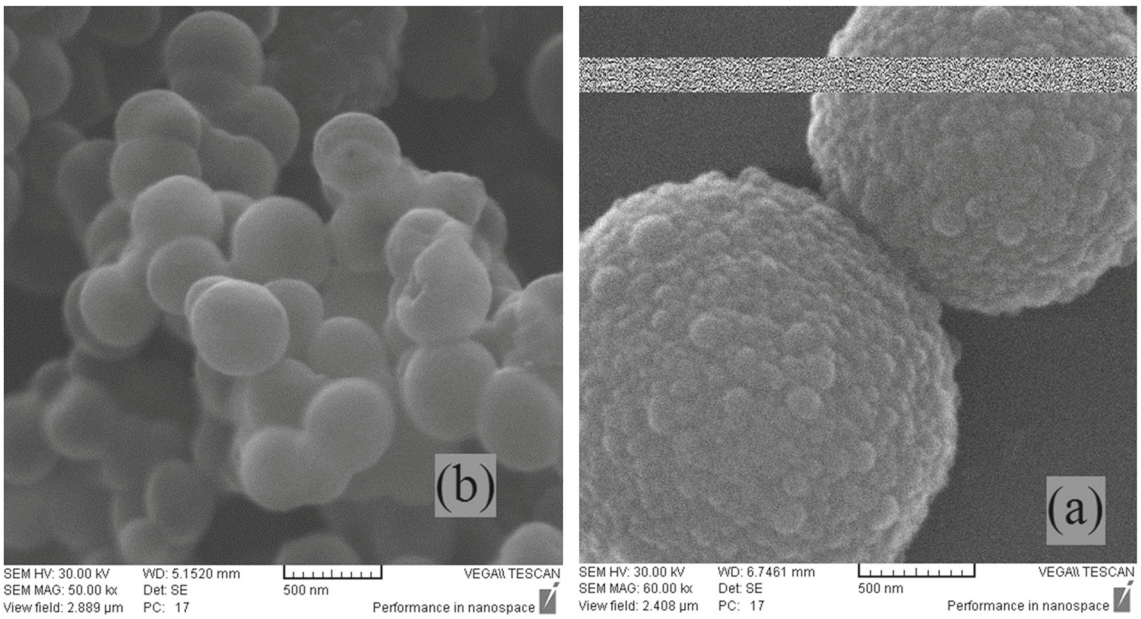

Fig. 5 SEM images of C@SiO_2 **a** before and **b** after calcination

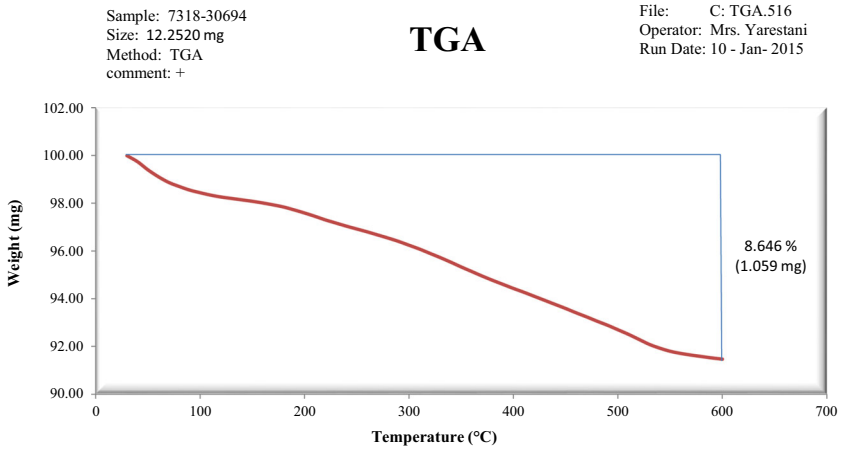

Fig. 7 TG curve of C@SiO_2@APTES

3.1.1 Effect of Concentration

SEM images of Fig. 1a and b are related to two samples with the same synthesis procedure and only different in glucose concentration. It was found that for uniform carbon spheres, the optimal concentration of glucose monohydrate solution is 0.4 M, because nanospheres obtained at higher concentrations are agglomerated. SEM images in Fig. 1 show that samples at glucose concentration of 0.4 M contain carbon nanospheres more uniform and separated, but in 0.6 M glucose, nanospheres are agglomerated and become unsuitable templates for producing hollow nanospheres.

3.1.2 Effect of Time

SEM images in Fig. 2a–d are related to the four samples with the same synthesis procedures, differing only in reaction time. The time parameter is also an important factor in the synthesis of carbon nanospheres, because it is a polymerization reaction, and if the time is insufficient, a major part of it was converted to unreactive monomers or led to very small and non-uniform distributed nanospheres. To obtain the separated carbon nanospheres, the optimal time is 12 h. If the time increases, agglomeration occurs and if the time decreases, the growth of nanospheres is not completed and some of glucose particles remains non-spherical.

3.1.3 Effect of Temperature

SEM images in Fig. 3a–c are attributed to three samples prepared in different temperatures, 150, 180 and 210 °C. The best temperature for synthesis of these nanospheres was estimated 180 °C. Because at higher temperatures, the samples were agglomerated samples and at lower temperatures, complete reaction does not take place.

3.2 FT-IR Spectrum of Carbon Nanospheres

FT-IR spectroscopy was used to confirm the chemical bonds. According to Fig. S1 of ESI, it can be noted that in different times and temperatures of hydrothermal reaction, significant changes were not created in surface functional groups of carbon nanospheres. The more the time of reaction, the smaller the peak intensity in the region of 3400 cm^{-1}, representing a loss of more water [12]. Figure S1 shows the FT-IR spectrum of carbon nanospheres. The observed bands at 1620 and 1695 cm^{-1} are related to C=C and C=O stretching vibrations, respectively. The bonds are

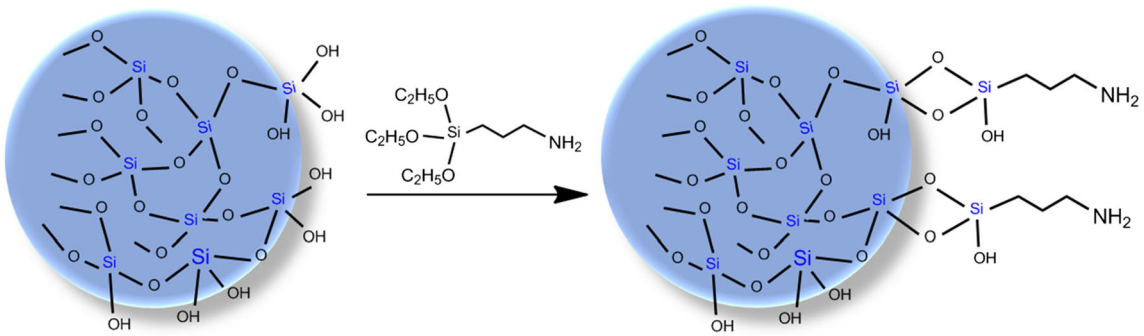

Scheme 2 Functionalization of SiO_2 spheres by APTES

created as a result of glucose aromatization process during hydrothermal reaction have been created. The decrease of frequency may be caused by the hydrogen bonding between the hydroxyl group and oxygen of carbonyl groups. The peaks at 1000-1400 cm^{-1} are attributed to stretching vibrations of C–OH and bending of OH, respectively, of course the broad peak in the range of 3400 cm^{-1} confirms that there are hydroxyl groups covalently bonded to the surface of spheres.

3.3 SEM Images of Core/Shell Nanostructures

SEM images in Fig. 4a and b are related to calcination of C@SiO_2 at 650 and 600 °C. To remove carbon spheres and organic parts from SiO_2, the optimum temperature were determined 500 °C. The SEM images of C@SiO_2 before and after calcination are illustrated in Fig. 5a and b. It seems that good nanospheres obtained at this temperature and they are suitable for drug release. At temperature less than 500 °C, the pores of sample are not suitable for the absorption of the drug. Above 500 °C, nanospheres are broken and converted into nanoparticles.

3.4 FT-IR Spectrum of Nanospheres Core/Shell

3.4.1 C@SiO_2 before Calcination

The FT-IR spectrum of C@SiO_2 before calcination is given in Fig. S2 of ESI. The observed bands at 462 and 1099 cm^{-1} are related to Si–O bending and Si–O stretching vibrations respectively, which represents the synthesis of SiO_2. Due to strong interaction of carbonyl group with silicon, carbonyl bond has converted to a single bond, and creates an additional peak in the range of 1100 cm^{-1}, which belongs to C–O stretching frequencies. Also, the peak intensity was reduced in the range of 1600 cm^{-1} [13].

3.4.2 C@SiO_2 after Calcination

Figure S3 of ESI shows the FT-IR spectrum of C@SiO_2 after calcination. The observed bands at 462 and 1099 cm^{-1} correspond to Si–O bending and Si–O stretching vibrations, respectively and represent removal of organic parts from SiO_2 [14].

3.4.3 FT-IR Spectrum of APTES

In Fig. S4 of ESI, the observed bands at 2935 cm^{-1} is attributed to C–H stretching vibrations of CH_2 group of propyl chain and represents attaching of aminopropyltriethoxysilane on the surface. The observed band in the range of 1020-1220 cm^{-1} is related to C–N stretching vibrations which covered by a broad peak related to the asymmetric stretching vibration of Si–O–Si group [15].

Table 1 BET measurements for SiO_2

Nanoporous specific area	916.82 m^2/g
Pore size	3.72 nm
Absorption desorption diagram	mesopore type 4

3.5 Powder X-ray Diffraction Patterns of SiO_2

Figure 6 shows the X-ray diffraction pattern of SiO_2 nanoparticles. There is a broad peak at 2θ =23°, which is characteristic for amorphous SiO_2 [16].

3.6 Thermal Analysis of C@SiO_2 @APTES

The TG curve of C@SiO_2@APTES is shown in Fig. 7. In the TG curves, there are three weight losses. The initial weight loss observed up to 30-190 °C is attributed to physically adsorbed water molecules [17, 18]. The next weight loss occurred at 190-350 °C which was related to surface groups of OH or in the other words, chemically absorbed water molecules [19]. The latest weight loss observed up to 350-600 °C is attributed to propyl chain [20]. Formation of SiO_2 nanoparticles modified with aminopropyltriethoxysilane are illustrated in Scheme 2.

3.7 Textural Properties of SiO_2 Nanospheres

The textural properties such as surface area and pore volume of SiO_2 nanospheres are given in Table 1. According to the

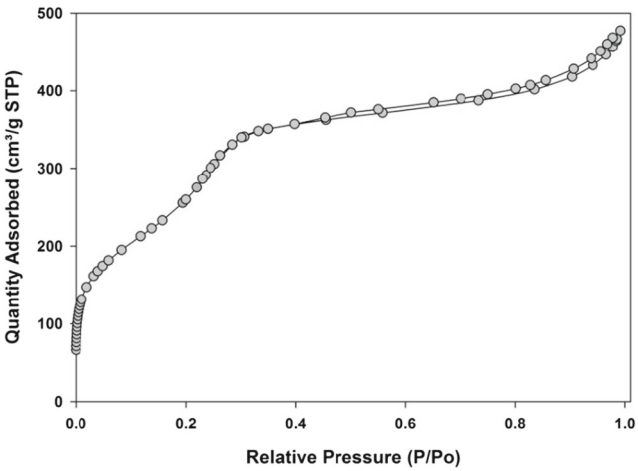

Fig. 8 N_2 adsorption/desorption isotherms of SiO_2 nanospheres

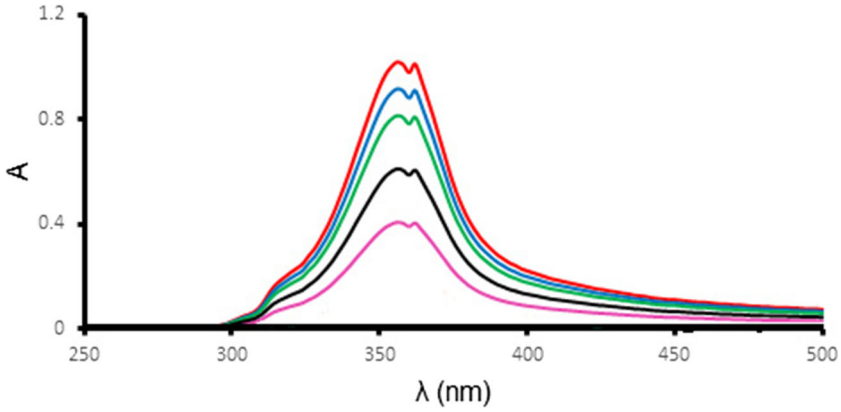

Fig. 9 UV-Vis absorption spectrum of solution of dexamethasone (250 ppm) and SiO_2 nanospheres: 0 (the bottom curve), 1, 2, 6 and 12h (top curve) after start of tests

results of BET measurements, it was found that synthesized SiO_2 containing porous structure of the mesoporous type. The specific surface area of SiO_2 nanospheres is 916.82 nm and the pore size is 3.72 nm, so it is desirable for the drug release [21]. The nitrogen adsorption–desorption isotherms obtained at 77 K are shown in Fig. 8. The isotherms obtained for the porous nanospheres are of Type IV, which is the characteristic feature of the mesoporous materials [9].

3.8 Drug Load and Release

3.8.1 Absorption of Drug by SiO_2 Nanospheres

To study the amount of drug absorbed by nanospheres and drug release in the simulated body fluid was applied UV-Vis absorption spectrum. By comparing the peak intensity of drug, efficiency of nanospheres in the drug absorption and release can be obtained. Figure 9 is related to UV-Vis absorption spectrum of dexamethasone solution (250 ppm) in the presence of SiO_2 nanospheres (0.01 g). Over time, the amount of drug absorption by nanospheres is increased. It should be noted that in this test, pH was 6 and is not used no acidic or alkaline agent to alter and control of pH. Molecular structure of dexamethasone is brought in Scheme 1. The $\pi \rightarrow \pi^*$ and $n \rightarrow \pi^*$ was the most likely transition.

3.9 Absorption of Drug by SiO_2 Nanospheres Modified with Aminopropyltriethoxysilane

Absorption spectrum of SiO_2 nanospheres modified with aminopropyltriethoxysilane is similar to the spectrum of SiO_2 nanospheres, only the difference is that the amount of drug absorbed by SiO_2 nanospheres modified with aminopropyltriethoxysilane is more than SiO_2 nanospheres. Figure 10 shows UV-Vis absorption spectrum of solution of drug (250 ppm) and SiO_2 nanospheres modified with aminopropyltriethoxysilane. Figure 11a and b show the amount of drug absorbed by SiO_2 nanospheres and SiO_2 nanospheres modified with aminopropyltriethoxysilane.

3.10 Study of Drug Release in SBF

In order to study the drug release absorbed by SiO_2 nanospheres modified with aminopropyltriethoxysilane and SiO_2 nanospheres were used the simulated body fluid. The solution containing 250 ppm of dexamethasone drug (50 mL) and porous nanospheres (0.01 g) were stirred for 72 h. After separation of nanospheres by centrifuge and washing with acetone, final product dried in a vacuum oven at 40 °C for 3 h. Obtained nanospheres were poured in SBF (100 mL) and placed at 37 °C. The amount of

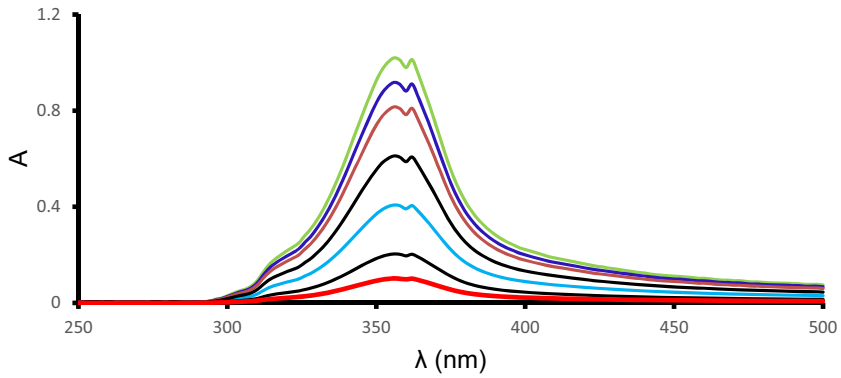

Fig. 10 UV-Vis absorption spectrum of solution of drug (250 ppm) and SiO_2 nanospheres modified with aminopropyltriethoxysilane 0 (the bottom curve), 1, 2, 6, 12, 24 and 48h (the top curve) after starting the tests

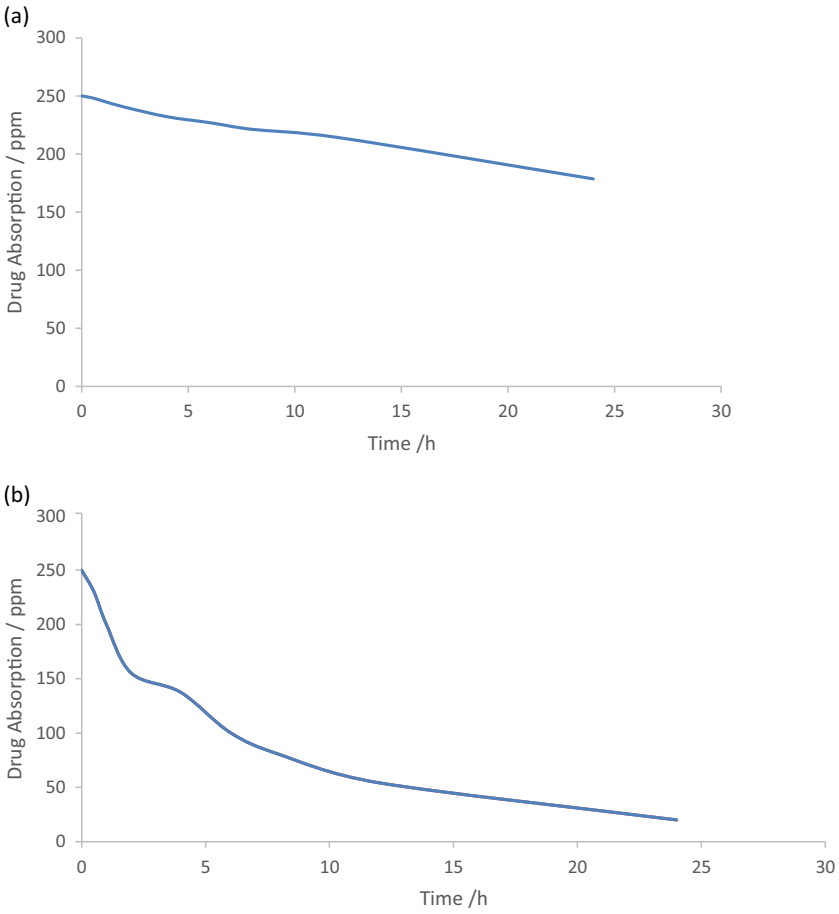

Fig. 11 Graph of the amount of drug absorbed by **a** SiO_2 nanospheres **b** SiO_2 nanospheres modified with aminopropyltriethoxysilane vs. time

drug release from nanospheres into simulated body fluid was sampled at different times. After separation of the loaded nanospheres using centrifugation for 20 minutes at 6000 rpm, UV-Vis absorption spectra of the loaded drug from the remaining solution were measured in the range 250 to 500 nm. UV-Vis absorption spectra related to the release of dexamethasone from SiO_2 nanospheres modified with aminopropyltriethoxysilane and SiO_2 nanospheres at different times are illustrated in Fig. 12. As seen in the figure, an increase in the intensity of absorption is related to increased concentrations of dexamethasone in simulated body fluid. It is noteworthy that no difference in the peak related to UV-Vis molecular absorption spectra of drug release from SiO_2 nanospheres modified with

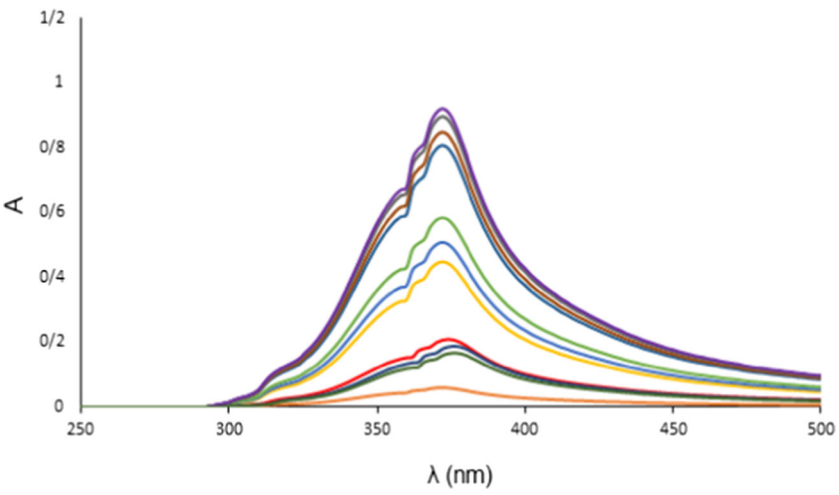

Fig. 12 UV-Vis absorption spectra of dexamethasone release from SiO_2 nanospheres modified with aminopropyltriethoxysilane: 0 (the bottom curve) 1, 2, 6, 12, 24, 48 and 72 h (the top curve) after starting

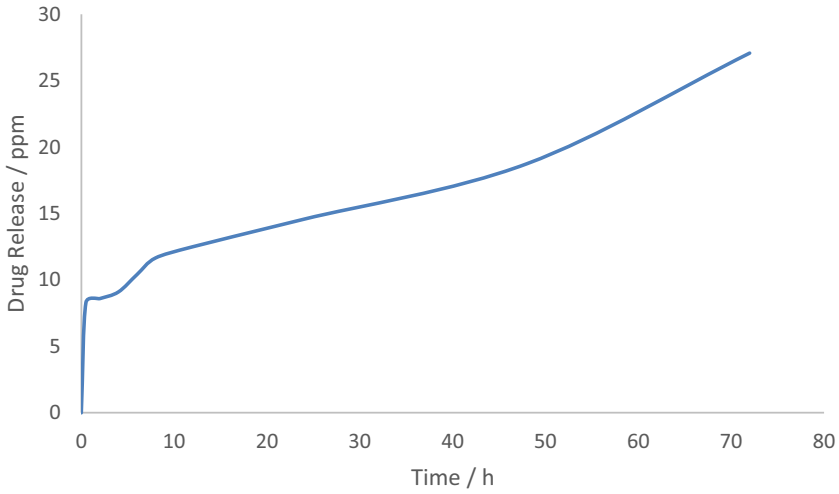

Fig. 13 Graph of the release of dexamethasone drug from SiO_2 nanospheres modified with aminopropyltriethoxysilane in SBF versus time

aminopropyltriethoxysilane and SiO_2nanospheres were not observed. Figure 13 shows the amount of drug release from nanospheres in SBF and also drug release lasted for 72 hours.

4 Conclusions

In this work, hollow mesoporous silica (HMS) spheres were synthesized using glucose as a carbon precursor and CTAB. The SiO_2 nanoparticles were functionalized using aminopropyltriethoxysilane. Obtained mesoporous material was studied for the load and release of a drug. The amount of drug adsorption was increased with functionalizing of SiO_2 nanospheres and drug release lasted for 72 hours. Synthesized carriers do not need to adjust pH for absorption and release of the drug and this is considered as an advantage.

Acknowledgements The authors are grateful to the financial support of Iran University of Science and Technology.

References

1. Chen X, Kierzek K, Jiang Z, Chen H, Tang T, Wojtoniszak M, Kalenczuk RJ, Chu PK, Borowiak-Palen E (2011) Synthesis, growth mechanism, and electrochemical properties of hollow mesoporous carbon spheres with controlled diameter. J Phys Chem C 115:17717
2. Chen Y, Chen H, Shi J (2014) Construction of homogeneous/heterogeneous hollow mesoporous silica nanostructures by silica-etching chemistry: principles, synthesis, and applications. J Acc Chem Res 47(1):125
3. Qiao SZ, Lin CX, Jin Y, Li Z, Yan Z, Hao Z, Huang Y (2009) Lu GQ(M). Surface-functionalized periodic mesoporous organosilica hollow spheres. J Phys Chem C 113(20):8673
4. Teng Z, Su X, Zheng Y, Sun J, Chen G, Tian C, Wang J, Li H, Zhao Y, Lu G (2013) Mesoporous silica hollow spheres with ordered radial mesochannels by a spontaneous self-transformation approach. Chem Mater 25(1):98
5. Parambadath S, Rana VK, Moorthy S, Chu S, Park S, Lee D, Sung G, Ha C (2011) Periodic mesoporous organosilicas with co-existence of diurea and sulfanilamide as an effective drug delivery carrier. J Solid State Chem 184(5):1208
6. Zhu Y, Jian D, Wang S (2011) Investigation of loading and release of guest molecules from hollow mesoporous silica spheres. Micro Nano Lett 6(9):802
7. Lin CX(C), Qiao SZ, Yu CZ, Ismadji S, Lu GQ(M) (2009) Periodic mesoporous silica and organosilica with controlled morphologies as carriers for drug release. J Micropor Mesopor Mat 117:213
8. Zhang L, Feng X, Liu H, Qian D, Zhang L, Yu X, Cui F (2004) Hydroxyapatite/collagen composite materials formation in simulated body fluid environment. J Mater Lett 58(5):719
9. Sasidharan M, Bhaumik A (2013) Novel and mild synthetic strategy for the sulfonic acid functionalization in periodic mesoporous ethenylene-silica. J Appl Mater Interfaces 5:2618
10. Moorthy MS, Park S, Fuping D, Hong S, Selvaraj M, Ha C (2012) Step-up synthesis of amidoxime-functionalised periodic mesoporous organosilicas with an amphoteric ligand in the framework for drug delivery. J Mater Chem 22:9100
11. Luo Y, Yang P, Lin J (2008) Synthesis and characterization of urea bridged hybrid periodic mesoporous organosilica materials. Micropor Mesopor Mat 111:194
12. Sevilla M, Fuertes AB (2009) The production of carbon materials by hydrothermal carbonization of cellulose. J Carbon 47(9): 2281
13. Luigi R, Francesco C, Raffaele C, Ilaria R (2011) A mechanochemical approach to porous silicon nanoparticles fabrication. J Mater 4(6):1023
14. Nakamoto K (2009) Infrared and raman spectra of inorganic and coordination compounds Part B, 6th edn. Wiley, New Jersey
15. Sadtler SP (1978) Handbook of infrared spectra. Bio-Red Laboratories
16. Tadjarodi A, Haghverdi M, Mohammadi V (2012) Preparation and characterization of nano-porous silica aerogel from rice husk ash by drying at atmospheric pressure. J Mater Res Bull 47:2584
17. Moritz M, Geszke-Moritz M (2015) Mesoporous silica materials with different structures as the carriers for antimicrobial agent.

Modeling of chlorhexidine adsorption and release. J Appl Surf Sci 356:1327
18. Saikia L, Srinivas D, Ratnasamy P (2006) Chemo, regio- and stereo-selective aerial oxidation of limonene to the endo-1,2-epoxide over Mn(Salen)-sulfonated SBA15. J Appl Catal A-Gen 309:144
19. Bagherzadeh M, Zare M, Amini M, Salemnoush T, Akbayrak S, Özkar S (2014) Epoxidation of olefins catalyzed by a molybdenum-Schiff base complex anchored in the pores of SBA-15. J Mol Catal A-Chem 395:470
20. Perez-Quintanilla D, Sanchez A, Del Hierro I, Fajardo M, Sierra I (2009) Preconcentration of Zn(II) in water samples using a new hybrid SBA-15-based material. J Hazard Mater 166:1449
21. Jaeger DA, Reddy VB, Bohle DS (1999) Cleavable double-chain surfactant Co(III) complexes. Tetrahedron Lett 40(4):649